

# A Novel Switchable Dielectric Bandpass Filter with Reconfigurable Transmission Zeros

Liangzu Cao<sup>\*</sup>, Di Deng, Shuai Wu, Junmei Yan, and Lixia Yin

**Abstract**—This paper proposes a new method to produce and reconfigure transmission zero(s) (TZ(s)). The TZs are constructed by using lumped elements in series with dielectric resonators, which is different from conventional methods such as introducing a cross coupling between nonadjacent resonators and mixed coupling between adjacent resonators. The proposed filter consists of two dielectric resonators, a capacitor, an inductor, two PIN diodes, etc. Two PIN diodes are used as switches to realize reconfigurable TZ(s). The mechanism is analyzed theoretically. An equivalent schematic diagram is simulated by using ADS software. The simulated results show that the structure can realize four response states, i.e., no TZ in the stopband, one TZ in the lower stopband, one TZ in the upper stopband, and two TZs in both sides of the stopband of the filter, respectively. The dielectric resonators (DRs) were made of dielectric ceramics with high dielectric constant of about 92. The filter was fabricated on a dielectric substrate and measured by using a vector network analyzer and double regulated DC power supply.

## 1. INTRODUCTION

Tunable/switchable filters have been widely used in modern communication systems due to their potential to reduce volume and design complexity. Many tunable microstrip bandpass filters with center frequency or/and in-band bandwidth control have been published [1–4], and there are some articles about the bandpass filters with reconfigurable or controllable TZ(s) [5–10]. In [5], one switchable TZ is realized by only tuning the resonant frequencies of waveguide resonators. In [6], the reconfiguration of TZs of a third-order cross coupled openloop bandpass filter is realized by changing the ratio of the two capacitances to tune coupling coefficient and the sign of coupling coefficient, which makes the transmission zero of the filter locate at either high side or low side of the passband. In [7], a reconfigurable asymmetric frequency response bandpass filter using a dual-mode open-loop resonator was demonstrated experimentally, and two cases are designed by controlling the resonant frequencies of the odd-mode and even-mode. The positions of TZs are the same as [6]. In [8], one TZ of a three-pole tunable combline bandpass filter can be controlled by a varactor loaded I/O network, and the TZ can be tuned from 1.37 to 1.64 GHz in the lower stopband of the filter. In [9], two TZs can be tuned by a piezoelectric transducer. In [10], the reconfiguration of TZs of a third-order combline filter is realized by using four varactors, but only two states were implemented by adjusting four dc bias voltages. In [11], the TZ can be specified at the lower or higher passband edge by controlling the even- and odd-mode resonant frequencies. But the methods mentioned above to reconfigure TZs can only achieve two states, i.e., one TZ in either lower or higher stopband.

This paper designs a second-order bandpass filter with reconfigurable TZs, and the TZs can be controlled by two PIN diodes. Four cases are realized, including no TZ in the stopband (conventional chebyshev response), one TZ in the lower stopband, one TZ in the upper stopband, and two TZs in

---

*Received 6 January 2022, Accepted 15 February 2022, Scheduled 24 February 2022*

<sup>\*</sup> Corresponding author: Liangzu Cao (clz4233@aliyun.com).

The authors are with the School of Mechanical and Electronic Engineering, Jingdezhen Ceramic Institute, Jingdezhen 333403, China.

both sides of the stopband of the proposed filter. The prototype was made of two DRs to validate the design concept.

**2. DESIGN PROCEDURE**

Figures 1(a) and (b) show the design schematic diagrams of the proposed filter and a conventional filter with cross coupling between the source and load, where  $C_k$  and  $L_k$  ( $k = 1, 2$ ) form a parallel resonator;  $J_{i,i+1}$  ( $i = 0 \sim 2$ ) is a admittance inverter which represents the coupling between the source/load and a resonator or the inter-stage coupling; and  $x_1$ ,  $x_2$ , and  $x_{SL}$  are lumped elements.

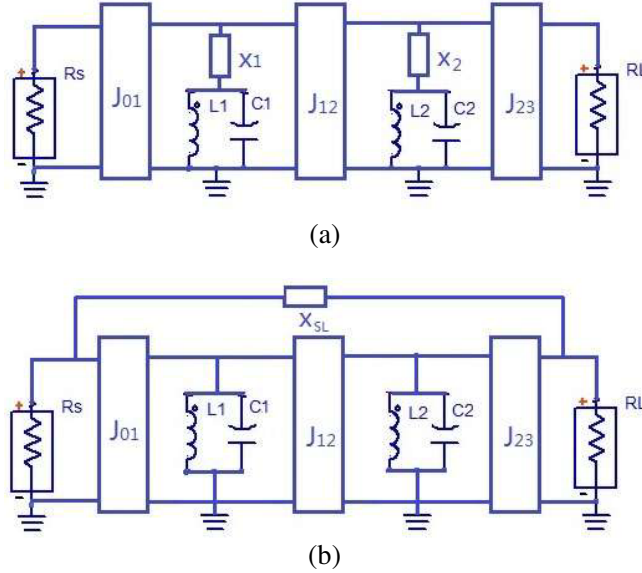


**Figure 1.** Schematic diagrams of the proposed and conventional filters. (a) The proposed filter. (b) Conventional filter with cross coupling between source and load.

For Fig. 1(b), two TZs can be produced in the lower and upper stopbands when the phase differences between two paths are equal to  $\pi$  below resonance and above resonance [12].

But for Fig. 1(a), there are many cases depending on the property of the lumped elements  $x_1$  and  $x_2$ . We analyze in detail the conditions that produce TZs.

Figure 2 plots a single resonant cell weakly coupled to the input and output ports. The element  $x_1$  can be defined as a resistor, a capacitor, or an inductor, and its frequency response is different.

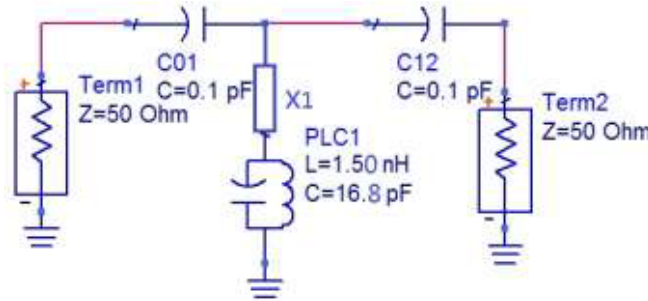


**Figure 2.** A single resonant cell.

For Fig. 2,  $ABCD$ -matrix is as follows,

$$\begin{aligned} F &= A_1 \cdot A_2 \cdot A_3 = \begin{pmatrix} 1 & Z_{c01} \\ 0 & 1 \end{pmatrix} \begin{pmatrix} 1 & 0 \\ 1/Z_{in} & 1 \end{pmatrix} \begin{pmatrix} 1 & Z_{c12} \\ 0 & 1 \end{pmatrix} \\ &= \begin{pmatrix} Z_{c01}/Z_{in} + 1, & Z_{c01} + Z_{c12} \cdot (Z_{c01}/Z_{in} + 1) \\ 1/Z_{in}, & Z_{c12}/Z_{in} + 1 \end{pmatrix} \end{aligned} \quad (1)$$

where  $Z_{c01}$ ,  $Z_{c12}$ , and  $Z_{in}$  are the impedances of input capacitor  $C_{01}$ , output capacitor  $C_{12}$ , and the resonator loaded with a lumped element  $x_1$ , and  $Z_{in}$  is expressed as,

$$Z_{in} = x_1 + \frac{1}{j(\omega C_1 - 1/\omega L_1)} \quad (2)$$

For a capacitor, resistor, and an inductor,  $x_1$  is equal to  $1/j\omega C$ ,  $j\omega L$ , and  $R$ , respectively.

The scattering parameter  $S_{21}$  given below is derived from the relationship between  $S$  matrix and  $ABCD$  matrix:

$$S_{21} = \frac{2}{A + B/Z_0 + C \cdot Z_0 + D} \quad (3)$$

where  $A$ ,  $B$ ,  $C$ , and  $D$  are the elements of  $ABCD$  matrix shown in Eq. (1), and  $Z_0$  is the system impedance,  $50 \Omega$ .

Given the parameters of the elements in Fig. 2, the magnitude of  $S_{21}$  can be obtained based on Eq. (3), but it is complicated. Here, we only analyze the position of TZ for a different lumped element  $x_1$ .

Substituting Eq. (1) into Eq. (3) and simplifying, we can obtain Eq. (4),

$$S_{21} = \frac{100Z_{in}}{100(Z_{in} + Z_{C01}) + Z_{C01}(2Z_{in} + Z_{C01}) + 2500} \quad (4)$$

For convenience, set  $Z_{c01} = Z_{c12}$  in math operation.

When  $|S_{21}| = 0$ , the denominator of Equation (4) is a complex whose absolute value is more than zero, i.e.,  $|Z_{in}| = 0$ , TZ can be produced.

If  $x_1 = j\omega L$ ,  $Z_{in} = j\omega L + \frac{j\omega L_1}{1 - (\omega/\omega_0)^2}$ , and  $|Z_{in}| = 0$ , then,

$$\left(\frac{\omega}{\omega_0}\right)^2 = 1 + \frac{L_1}{L}, \quad (5)$$

It is stated that  $\omega > \omega_0$  and the TZ is at the right side of the resonant peak. The larger the inductance of  $L$  is, the closer the TZ is to the resonant peak.  $\omega_0$  is a resonant frequency of the LC parallel circuit.

If  $x_1 = 1/j\omega C$ ,  $Z_{in} = 1/j\omega C + \frac{1}{j\omega C_1[1 - (\omega_0/\omega)^2]}$ , and  $|Z_{in}| = 0$ , then,

$$\left(\frac{\omega_0}{\omega}\right)^2 = 1 + C/C_1, \quad (6)$$

It is stated that  $\omega < \omega_0$  and the TZ is at the left side of the resonant peak. The larger the capacitance of  $C$  is, the farther the TZ is from the resonant peak.

If  $x_1 = R$ ,  $|Z_{in}| \neq 0$ , there is no TZ.

Figure 3 shows the simulated responses by using ADS software. It can be seen that a resonant peak of 1 GHz occurs in three cases. A TZ in the upper stopband appears in the case loaded with an inductor, and a TZ in the upper stopband appears in the case loaded with a capacitor and no TZ in the case loaded with a resistor.

Based on the above analysis, we design a switchable bandpass filter with reconfigurable TZs. Fig. 4 shows the equivalent circuit of the proposed filter.  $C_{i,i+1}$  ( $i = 0 \sim 2$ ) is a coupling capacitor between the source/load and the resonant cell or two cells.  $C_{11}$  and  $L_{22}$  are the inductor and capacitor loaded at the end of LC resonators, respectively.  $K_1$  and  $K_2$  are switches.

The performances of the proposed filter without TZ are as follows. Center frequency is 785 MHz, with 3 dB bandwidth 70 MHz, and the order of the filter is 2.

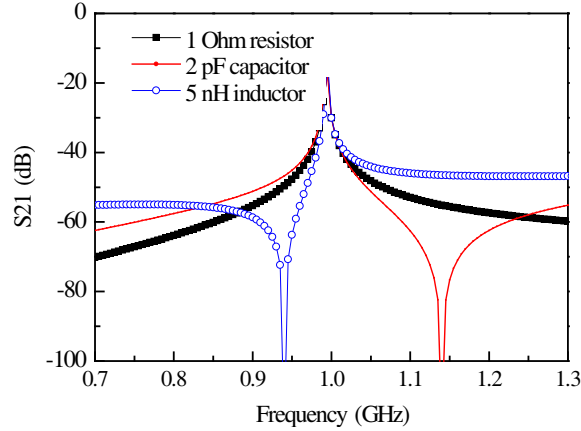


**Figure 3.** The transmission responses of the LC resonator loaded different elements.

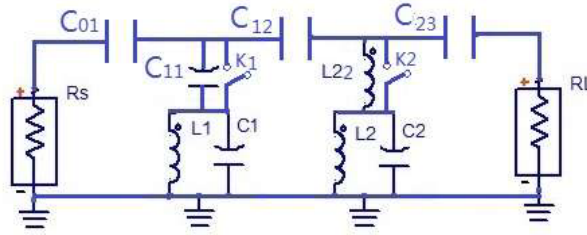


**Figure 4.** Equivalent circuit of the proposed filter.

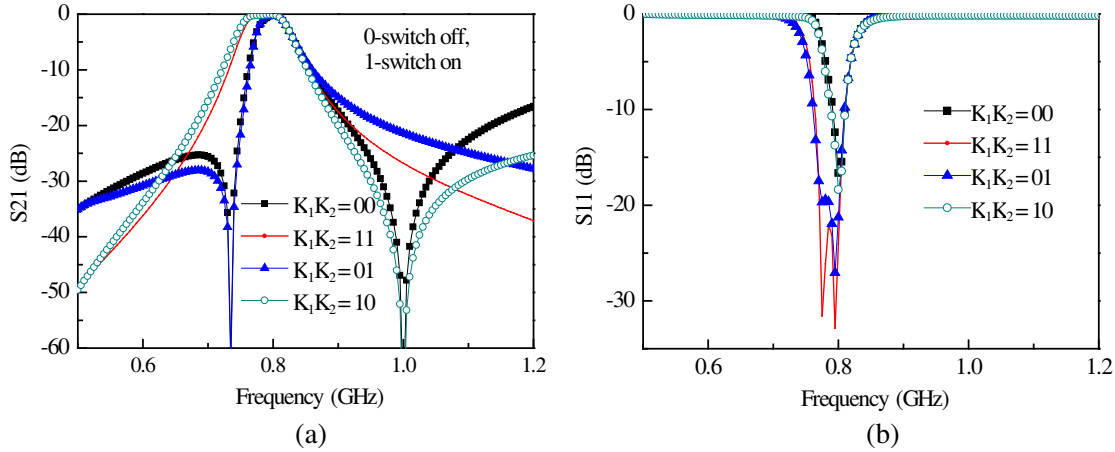


**Figure 5.** Simulated responses of the filter with four states. (a) Transmission responses. (b) Reflection responses.

The filter design is based on a Chebyshev lowpass prototype with a ripple of 0.1 dB. The LC parallel circuits are realized by coaxial dielectric resonators with a characteristic impedance of  $8\ \Omega$  and a dielectric constant of 92. The structure parameters can be determined by the required coupling coefficient and external quality factor [13], and optimized by ADS software. The optimized parameters are as follows. The length of the DR is 9.5 mm,  $C_{01} = 2.5\ \text{pF}$ ,  $C_{12} = 1.2\ \text{pF}$ ,  $C_{11} = 10\ \text{pF}$ ,  $L_{22} = 5\ \text{nH}$ .

Figure 5 shows the simulated responses of the filter under the conditions of switches with four combinations. There are four cases, i.e., no TZ in the stopband (conventional Chebyshev response), one TZ in the lower stopband, one TZ in the upper stopband, and two TZs in both sides of the stopband of the filter, respectively.

### 3. EXPERIMENTAL RESULTS

DRs are used to realize LC parallel resonant circuits, and PIN diodes are used as switches. Fig. 6 shows the layout of the filter, and the effective size is about  $15\text{ mm} \times 20\text{ mm} \times 6.5\text{ mm}$ . In Fig. 6,  $R_b$  and  $L_b$  form a biased circuit for blocking RF leakage, and  $k_1$  and  $k_2$  are switches. The pad marked with  $V_c$  is used to connect a DC supply, and other symbols are the same as that of Fig. 4.

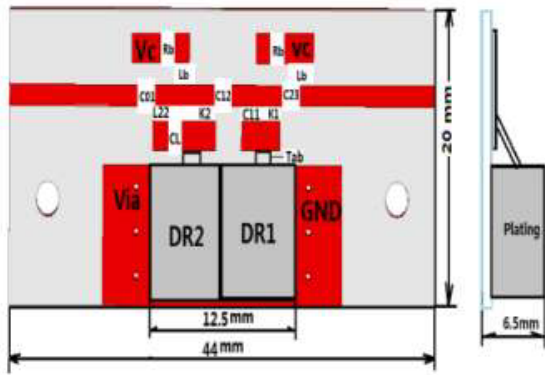


Figure 6. The layout of the proposed filter.

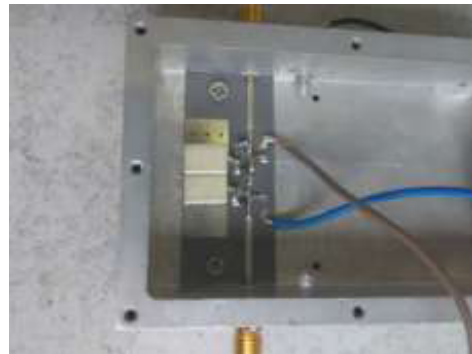


Figure 7. Photo of the proposed filter.

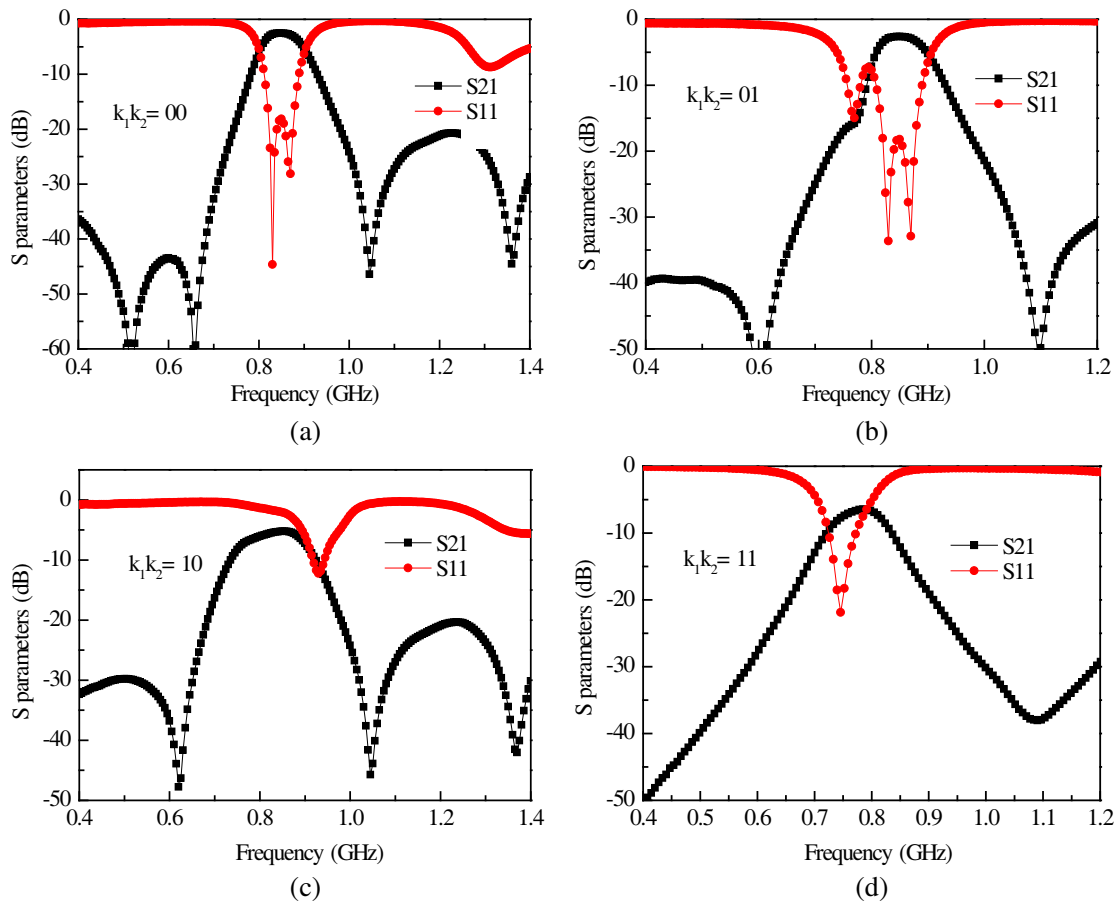


Figure 8. Measured frequency responses. (a) Both switches are off. (b)  $k_1$  off and  $k_2$  on. (c)  $k_1$  on and  $k_2$  off. (d) Both switches are on.

The DRs are made of dielectric ceramics with dielectric constant of 92,  $Q \times f$  value of more than 3000 GHz, and near zero frequency temperature coefficient, and their physical dimensions of the DR are a side length of 6 mm, an inner diameter of 1.8 mm, and a height of 8.8 mm. The PIN diodes are BAR63-02 from Infineon, and lumped elements are 0603 types from Murata Co., LTD. The capacitances of the coupling capacitors  $C_{01}$  and  $C_{12}$  are equal to 2.3 pF and 1.5 pF, respectively. The capacitance of the capacitor loaded at the open end of the DR is 4 pF. The inductance of the inductor loaded at the open end of the DR is 5 nH, and the capacitance of the capacitor in series with this inductor is 20 pF. Two chip resistors of 1 k $\Omega$  in series with two inductors of 27 nH are used in biased circuits for blocking RF leakage. The filter was fabricated on a dielectric substrate with a dielectric constant of 2.55 and a thickness of 0.5 mm, and measured by using network analyzer E5071B.

Figure 7 is a photo of the proposed filter. The measured parameters are presented in Fig. 8. The measured results show that the proposed filter has four frequency responses when the switches are on or off. It is observed that there are some differences between simulated and measured results due to the lumped elements loaded to DRs and the combline structure, which results in extra TZs. According to our preliminary analysis, the lower extra TZ may be the self-resonance generated by the series resonant branch which is loaded to the DR for producing TZ in the upper stopband, while the upper extra TZ is the inherent TZ of the combline filter. Further work needs to be done to eliminate the lower extra TZ. The higher insertion loss of the filter in the case of both switches on attributes to the on-resistance of PIN.

#### 4. CONCLUSIONS

A switchable second-order dielectric bandpass filter with reconfigurable TZs has been developed. A dielectric coaxial resonator loaded with an inductor or a capacitor can produce a TZ which is located in the upper or lower stopband. A switch is parallel with the loaded inductor or capacitor to realize four frequency responses. The insertion losses of the proposed filter are poor due to the on-resistance of PIN diodes and parasitic resistances of the lumped elements. The next goal is to improve the performances of the filter in each state.

#### ACKNOWLEDGMENT

This work was supported by the Educational Commission of Jiangxi Province of China [No. GJJ201305], College Student Innovation and Entrepreneurship Project (provincial level).

#### REFERENCES

1. Cao, L., L. Wang, and L. Yin, "Progress in electrically tunable microwave bandpass filters," *Electronic Components & Materials in Chinese*, Vol. 27, No. 2, 9–17, 2019.
2. Lan, B.-Z., Y. Qu, C.-J. Guo, et al., "A fully reconfigurable bandpass-to-notch filter with wide bandwidth tuning range based on external quality factor tuning and multiple-mode resonator," *Microw. Opt. Technol. Lett.*, Vol. 61, No. 5, 1253–1258, 2019.
3. Kingsly, S., M. Kanagasabai, M. G. N. Alsath, et al., "Compact frequency and bandwidth tunable bandpass-bandstop microstrip filter," *Microw. Wirel. Compon. Lett.*, Vol. 28, No. 9, 786–788, 2018.
4. Schuster, C., A. Wiens, F. Schmidt, et al., "Performance analysis of reconfigurable bandpass filters with continuously tunable center frequency and bandwidth," *IEEE Transactions on Microwave Theory and Techniques*, Vol. 65, No. 11, 4573–4584, 2017.
5. Lin, W., K. Zhou, and K. Wu, "Tunable bandpass filters with one switch-able transmission zero by only tuning resonances," *IEEE Microwave and Wireless Components Letters*, Vol. 31, No. 2, 105, Feb. 2021.
6. Fu, M., Q. Feng, Q. Xiang, and N. Jiang, "Fully tunable filter with cross coupling and reconfigurable transmission zero," *Int. J. RF Microw. Comput. Aided. Eng.*, e22407, 2020.

7. Chun, Y.-H. and J.-S. Hong, "Electronically reconfigurable dual-mode microstrip open-loop resonator filter," *IEEE Microwave and Wireless Components Letters*, Vol. 18, No. 7, 449–451, Jul. 2008.
8. Chiou, Y.-C. and G. M. Rebeiz, "A tunable three-pole 1.5–2.2-GHz bandpass filter with bandwidth and transmission zero control," *IEEE Transactions on Microwave Theory and Techniques*, Vol. 59, No. 11, 2872–2878, 2011.
9. Cao, L. Z., Z.-J. Li, D. Deng, et al., "A tunable bandpass filter with bandwidth or transmission zeros control," *International Conference on Microwave and Millimeter Wave Technology*, 1–3, 2021.
10. Fathelbab, W. M. and M. B. Steer, "A reconfigurable bandpass filter for RF/microwave multifunctional systems," *IEEE Transactions on Microwave Theory and Techniques*, Vol. 53, No. 3, 1111–1116, 2005.
11. Tsai, H.-J., B.-C. Huang, N.-W. Chen, et al., "A reconfigurable bandpass filter based on a varactor-perturbed, T-shaped dual-mode resonator," *IEEE Microwave and Wireless Components Letters*, Vol. 24, No. 5, 297299, 2014.
12. Cao, L., J. Hu, and L. Yin, "Compact coaxial dielectric bandpass filter with load-source coupling," *2015 Asia-Pacific Microwave Conference (APMC)*, Vol. 2, 1–3, 2015.
13. Hong, J.-S., *Microstrip Filters for RF/Microwave Applications*, Wiley, New York, NY, USA, 2011.